Water Permeability of Polyunsaturated Lipid Membranes Measured by ^{17}O NMR

Daniel Huster,*# Albert J. Jin,§ Klaus Arnold,# and Klaus Gawrisch*
*Laboratory of Membrane Biochemistry and Biophysics, National Institute on Alcohol Abuse and Alcoholism, National Institutes of Health, Rockville, Maryland 20852 USA; #Institute of Medical Physics and Biophysics, University of Leipzig, 04103 Leipzig, Germany; and §Physical Sciences Laboratory, DCRT, National Institutes of Health, Bethesda, MD 20892 USA

ABSTRACT Diffusion-controlled water permeation across bilayers of polyunsaturated phospholipids was measured by ^{17}O nuclear magnetic resonance. In 100-nm extruded liposomes containing 50 mM $MnCl_2$, water exchange between internal and external solutions was monitored via changes in the linewidth of the ^{17}O water resonance of external water. Liposome size and shape were characterized by light scattering methods and determination of liposome trapped volume. At 25°C, the following water permeability coefficients were determined: 18:0–18:1n-9 PC, 155 ± 24 μm/s; 18:0–18:3n-3 PC, 330 ± 88 μm/s; and 18:0–22:6n-3 PC, 412 ± 91 μm/s. The addition of 1 M ethanol reduced permeability coefficients to 66 ± 15 μm/s for 18:0–18:1n-9 PC and to 239 ± 67 μm/s for 18:0–22:6n-3 PC. Furthermore, the addition of 50 mol% 18:1n-9–18:1n-9 PE reduced the water permeability from 122 ± 21 μm/s for pure 18:1n-9–18:1n-9 PC to 74 ± 15 μm/s for the mixture. The significant increase in water permeation for membranes with polyunsaturated hydrocarbon chains correlates with looser packing of polyunsaturated lipids at the lipid-water interface and the suggested deeper penetration of water into these bilayers. Ethanol may block water diffusion pathways by occupying points of water entry into bilayers at the interface. The addition of dioleoylphosphatidylethanolamine increases lipid packing density and, consequently, reduces permeation rates.

INTRODUCTION

Lipid bilayers are excellent dialysis membranes, representing an invincible obstacle for ion diffusion, but allowing rapid permeation of solutes such as water or ethanol. Water is known to permeate the membrane with relative ease, even in the absence of special water channels, allowing nature to regulate cell volume rapidly (Finkelstein, 1987).

Water permeability across lipid bilayers has been studied for more than 25 years by a variety of experimental methods (Disalvo et al., 1989; Finkelstein, 1987; Deamer and Bramhall, 1986; Fettiplace and Haydon, 1980). It was observed that rates of water permeation are higher for liquid crystalline lipids than for the gel state (Fettiplace and Haydon, 1980). Furthermore, water permeation depends on membrane lipid composition, e.g., lipid headgroups, chain length and unsaturation, and cholesterol concentration (Paula et al., 1996; Jansen and Blume, 1995; Koenig et al., 1992; Ye and Verkman, 1989; Spineni et al., 1983; Fettiplace and Haydon, 1980). It has been suggested that polyunsaturated membranes like those found in brain synaptosomes and the retina are particularly permeable to water, but their permeability coefficients have not been measured yet.

In recent studies conducted at our laboratory, the biophysical properties of a series of mixed-chain polyunsaturated lipids with one to six double bonds in the sn-2 chain have been investigated (Barry and Gawrisch, manuscript submitted for publication; Separovic and Gawrisch, 1996; Holte et al., 1995). We studied sn-1 chain order as a function of sn-2 chain unsaturation and concluded that polyunsaturated lipids occupy a larger area per lipid in the bilayer, which may ease penetration of water molecules (Holte et al., 1995). Looser packing of unsaturated lipids and, perhaps, deeper water penetration have been also detected by diffraction methods (Wiener and White, 1992; Simon and McIntosh, 1986). Furthermore, fluorescence measurements on polyunsaturated lipids revealed that water content in the bilayer hydrocarbon region increases with increasing chain unsaturation (Ho et al., 1995; Slater et al., 1993; Straume and Litman, 1987).

Ethanolamine headgroups result in phospholipid bilayers that are more tightly packed (Thurmond et al., 1991; Lafleur et al., 1990). Smaller cross-sectional areas in PC also result when PE is mixed with PC (Barry and Gawrisch, manuscript submitted for publication; Separovic and Gawrisch, 1996; Fenske et al., 1990; Lafleur et al., 1989, 1990). Following the previous argument that water permeability through membranes is strongly related to packing density of lipids, one would expect lower water permeability coefficients for mixed PC/PE compared to pure PC membranes.

Received for publication 8 January 1997 and in final form 21 April 1997.

Address reprint requests to Dr. Klaus Gawrisch, Laboratory of Membrane Biochemistry and Biophysics, National Institute on Alcohol Abuse and Alcoholism, National Institutes of Health, Rm. 158, 12420 Parklawn Dr., Rockville, MD 20852. Tel.: 301-594-3750; Fax: 301-594-0035; E-mail: gkl@cu.nih.gov.

Abbreviations used: 18:0–18:1 PC, 1-stearoyl-2-oleoyl-sn-glycero-3-phosphocholine; $16:0_{d31}$-18:1 PC, 1-palmitoyl$_{d31}$-2-oleoyl-sn-glycero-3-phosphocholine; 18:1–18:1 PC, 1,2-dioleoyl-sn-glycero-3-phosphocholine; 18:0–18:3 PC, 1-stearoyl-2-α-linolenoyl-sn-glycero-3-phosphocholine; 18:0–22:6 PC, 1-stearoyl-2-docosahexaenoyl-sn-glycero-3-phosphocholine; 22:6–22:6 PC, 1,2-didocosahexaenoyl-sn-glycero-3-phosphocholine; 18:1–18:1 PC, 1,2-dioleoyl-sn-glycero-3-phosphocholine; 18:1–18:1 PE, 1,2-dioleoyl-sn-glycero-3-phosphoethanolamine; L_α, lamellar liquid-crystalline phase; L_β, lamellar gel phase.

0006-3495/97/08/855/10 $2.00

The addition of ethanol may alter water permeation because of ethanol's influence on lipid order. Ethanol in lipid bilayers binds to the lipid-water interface region, including lipid phosphate groups, glycerol, and upper hydrocarbon chain regions (Holte and Gawrisch, 1997; Barry and Gawrisch, 1994, 1995). Interface binding increases separation between lipid molecules, which increases the motional freedom of lipid hydrocarbon chains (Barry and Gawrisch, 1994; Taraschi et al., 1985). Lower lipid order is expected to translate into higher water permeation rates. However, ethanol molecules compete with water for the same binding sites at the lipid-water interface and may interfere with water entry into bilayers. Water permeability of bilayers in the presence of ethanol has been investigated, but results from different laboratories appear to contradict each other. Whereas recent experiments on model membranes by Jansen and Blume (1995) and Lahajnar et al. (1995) found decreased water permeability in the presence of ethanol, previous investigations on cell membranes reported increased permeability (Inoue et al., 1985; Seeman et al., 1970).

Absolute membrane water permeability coefficients are measured with great difficulty. Relative differences in water permeability typically have good reproducibility, but absolute values measured at different laboratories by different experimental techniques may deviate, even in the order of magnitude (Haines and Liebovitch, 1995). This divergence reflects the hardship in calibrating a permeation measurement and, perhaps, specific membrane perturbations caused by the experimental approach.

Our NMR experiments on water permeation rely on paramagnetic ion-induced differences in water relaxation (Swift and Connick, 1962). The range of water permeation coefficients that can be measured with NMR depends critically on the magnitude of change in the relaxation rate. Fast water permeation, as in polyunsaturated lipids, requires particularly short relaxation times that are not accessible with the ^{1}H NMR signal of water at modest concentrations of paramagnetic ions. The ^{17}O NMR signal of water has exceptional sensitivity for spin-spin relaxation time, T_2, to Mn^{2+} concentration and is therefore better suited for measurements on polyunsaturated lipids. Isotopic enrichment is not required for most experiments because modern high- and medium-field spectrometers detect the ^{17}O NMR signal of water at natural abundance.

In most previous ^{17}O NMR experiments the relaxation time of water outside liposomes or cells was shortened and the exchange-mediated relaxation effect on trapped water inside the particles was measured (see, e.g., Haran and Shporer, 1976; Conlon and Outhred, 1972). This approach requires trapped water volumes of 10% or higher, which translates into very high lipid concentrations. A more suitable method is the one by Lipschitz-Farber and Degani (1980), which uses entrapped Mn^{2+} inside small sonicated vesicles. We modified the experiment by trapping the Mn^{2+} ions inside 100-nm extruded liposomes. This radius of curvature is large enough to prevent an influence from curvature on lipid packing but small enough to guarantee formation of single-walled unilamellar liposomes (Noy et al., 1995; Mui et al., 1993; Fenske and Cullis, 1993; Mayer et al., 1986). Calculated permeation rates depend on the precise determination of lipid concentration, liposome-trapped water volume, and liposome stability, which were investigated in parallel to the permeation experiments. At a concentration inside liposomes of 50 mM $MnCl_2$, permeability coefficients in the range of 50–1000 μm/s can be measured.

MATERIALS AND METHODS

Materials

18:0–18:1 PC, 16:0_{d31}-18:1 PC, 18:1–18:1 PC, 18:1–18:1 PE, and 22:6–22:6 PC were purchased from Avanti Polar Lipids (Alabaster, AL). The polyunsaturated lipids 18:0–18:3 PC and 18:0–22:6 PC were obtained from Matreya (Pleasant Gap, PA). Lipids were used without further purification. Lipid purity of the docosahexaenoic acid-containing lipids was checked by high-performance liquid chromatography, using a light scattering detector, and judged to be 98%. To prevent oxidation of lipids containing polyunsaturated fatty acids, the antioxidant butylated hydroxytoluene (BHT) was added at a molar lipid/BHT ratio of 250/1, and sample preparation and experiments were conducted with degassed solvents under an argon atmosphere. Anhydrous 200 proof ethanol was purchased from Pharmco Products (Brookfield, CT).

Sample preparation

18:0–18:1 PC, 16:0_{d31}-18:1 PC, and 18:1–18:1 PC were weighed into plastic vials as dry powders and hydrated as described below. Mixed PC/PE samples and polyunsaturated PCs were prepared from lipid chloroform or methylene chloride solutions. The organic solvent was removed under a stream of argon. The remaining lipid film was dispersed in water, frozen in liquid nitrogen, and lyophilized at a pressure of 100 μm Hg for a minimum of 8 h.

Liposome samples (1 wt%) were prepared in either 50 mM $MnCl_2$ to record the permeation process, or in a 72.9 mM NaCl solution (environment *A*, Fig. 1). The manganese-containing sample was used to measure T_2, and the sodium sample was used to determine T_{2A} (see Eq. 1). Both solutions yield an osmolarity of 134 ± 1 mOsmol/kg, as measured with the Advanced Osmometer 4995 (model 303; Advanced Instruments, Norwood, MA). Before extrusion, samples were freeze-thawed five times with liquid nitrogen. Unilamellar liposomes were produced by a three-step extrusion process through polycarbonate filters (Nuclepore Filtration Products, Cambridge, MA), using an extruder (Lipex Biomembranes, Vancouver, BC, Canada) operated with argon as previously described (Mayer et al., 1986; Hope et al., 1985). Dispersions were extruded three times through 400-nm filters, three times through 200-nm filters, and six times through 100-nm filters. Lipids extruded in either $MnCl_2$ or NaCl were dialyzed against a 72.9 mM NaCl solution in the same beaker for 20 h, using a double-sided biodialyzer (Sialomed, Columbia, MD). The solution was changed three times during dialysis. This procedure removes bulk manganese from solution while maintaining an identical ionic composition in the outer solution for both types of samples. For lipid species containing more than one double bond per chain, the entire sample preparation was carried out in an argon atmosphere.

Liposome size determination

The mean diameters and size distribution of extruded liposomes were determined by light scattering methods. Static and dynamic light scattering were measured on an instrument equipped with a BI-200SM goniometer, a BI-9000 AT digital correlator, and an argon ion laser (λ = 514.5 nm)

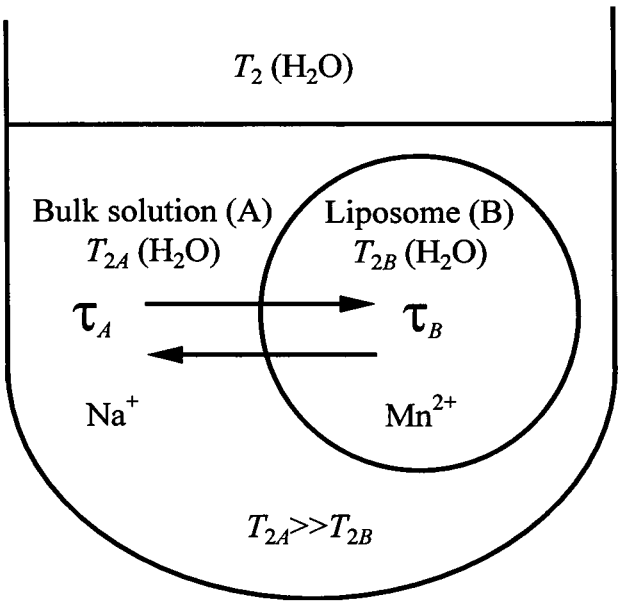

FIGURE 1 Water exchanges rapidly between a pool with long relaxation times on the outside of liposomes (*A*) and a pool inside the liposomes (*B*) with short NMR relaxation times due to 50 mM $MnCl_2$. Approximately 10^5 water molecules diffuse per second across the area occupied by one lipid. The effective relaxation time, T_2, is determined by the rate of water exchange between the two pools.

manufactured by Brookhaven Instruments Corp. (Holtsville, NY). Data for each sample were acquired in triplicate at angles of 30°, 45°, 60°, 90°, 120°, and 150° between incident and scattered light beams. The lipid concentration for this measurement was 0.01–0.1 wt%.

Measurement of trapped volume V_B

Liposomes extruded in the presence of electrolyte are reported to be nonspherical (White et al., 1996; Clerc and Thompson, 1994; Mui et al., 1993; Lichtenberg et al., 1981). Therefore, the hydrodynamic liposome diameter does not provide liposomal trapped volume. The amount of trapped water was calculated from the Mn^{2+} concentration in the extruded liposome dispersion after dialysis and liposome lysis by Triton X-100. The Mn^{2+} concentration was measured by a colorimetric Mn^{2+} assay (Spectroquant Manganese; Merck, Darmstadt, Germany). The NMR experiments gave no indication for Mn^{2+} leakage from the extruded liposomes. It was assumed that the Mn^{2+} concentration inside the liposomes did not change from the initial value of 50 mM during extrusion and dialysis.

Influence of Mn^{2+} on lipid packing

Samples of $16:0_{d31}$-18:1 PC, perdeuterated in the sn-1 chain, were prepared in H_2O, 50 mM $MnCl_2$, or 50 mM $CaCl_2$ solutions. Preparations were freeze-thawed and extruded as described above. After ultracentrifugation at 100,000 × *g* for 3 h, the pellet was transferred to glass tubes and freeze dried. Samples were rehydrated in deuterium-depleted water to the initial water content and equilibrated at 5°C for several days.

^2H NMR powder spectra were acquired on a Bruker DMX300 spectrometer (Bruker Instruments, Billerica, MA) at 46.1 MHz using a high power probe with a 5-mm solenoidal sample coil. A quadrupolar echo sequence (Davis et al., 1976) was used with two 1.8-μs 90° pulses and an interpulse delay of 50 μs. Between 10,000 and 30,000 scans were accumulated at a spectral width of 200 kHz.

Powder spectra were de-Paked according to the method of Sternin et al. (1983). The influence of Mn^{2+} on acyl chain order was evaluated by analyzing quadrupolar splittings.

Phospholipid concentration

After completion of measurements, the lipid concentration in the samples was determined by ^{31}P NMR. To obtain well-resolved isotropic resonance lines, lipids were solubilized in the detergent sodium dodecyl sulfate (400 mM) containing 0.1 mM EDTA. An aliquot of Na_2HPO_4 in D_2O was added to the sample for use as an internal ^{31}P intensity standard and to lock the magnetic field strength with a deuterium lock.

High-resolution ^{31}P NMR spectra were acquired on a Bruker DMX500 spectrometer (Bruker Instruments) operating at 202.4 MHz, using a spectrum width of 10 kHz. Phosphorus signals from lipid headgroups (PC, PE) and inorganic phosphorus were well separated (Colman and Gadian, 1976) and could be easily integrated by a peak-fitting procedure (Xedplot; Bruker Instruments).

Permeability measurement

The permeation process was treated as an exchange of water between two pools (Fig. 1), the external pool (*A*), with a long relaxation time (T_{2A}) and the internal (*B*), with a short relaxation time (T_{2B}) due to the presence of paramagnetic Mn^{2+} ions. The effective relaxation time, T_2, of external water depends on T_{2A}, T_{2B}, and the lifetime of water inside the liposomes, τ_B, according to

$$\frac{1}{T_2} = \frac{f}{T_{2B} + \tau_B} + \frac{1}{T_{2A}} \quad (1)$$

(Andrasko and Forsen, 1974; Swift and Connick, 1962). The ratio of internal to external water volume is given by the factor f ($f = V_B/V_A$). This equation assumes that resonance lines in environments *A* and *B* have the same chemical shift, confirmed experimentally for 18:0–18:1 PC. Furthermore, a size distribution of the liposomes modifies Eq. 1 in such a way that f and τ_B must be replaced by expressions that sum over all volume ratios, f_i, and lifetimes, τ_{Bi}, that occur according to the liposome size distribution function. This scenario was modeled and resulted in deviations of only 1–2% from permeability coefficients calculated from average values of f and τ_B. Therefore, the influence of size distribution was neglected.

High-resolution natural-abundance ^{17}O NMR spectra of water were accumulated on a Bruker DMX300 spectrometer at a resonance frequency of 40.7 MHz, using proton broadband decoupling. Typically, 1024 scans were accumulated with a repetition delay time of 100 ms. The relaxation times T_2 and T_{2A} were directly obtained from the Lorentzian fit of the lineshape. To determine the relaxation time of the internal water, T_{2B}, 10 mg of 18:0–18:1 PC was dispersed in 51.6 μl of 50 mM $MnCl_2$ solution, which yielded the same lipid-to-water ratio throughout the sample as inside the 100-nm unilamellar liposomes. The $MnCl_2$ solution contained 10% $H_2{}^{17}O$/90% H_2O (Cambridge Isotope Labs, Andover, MA) for detection of this severely broadened signal. The dispersion was freeze-thawed 10 times and stored for 2–3 days at 5°C for equilibration. T_{2B} was measured with a Hahn-echo pulse sequence with a between-pulse delay of 10 μs, using a solids probe. Free induction decays were left-shifted and Fourier transformed with a line broadening of 100 Hz. For comparison, T_{2B} was also obtained from a lineshape fit.

The permeability coefficient, P_d, was computed according to

$$P_d = \frac{V_B}{A\tau_B} \quad (2)$$

V_B is the internal volume of the liposomes, and *A* is their surface area. The trapped volume, V_B, was measured by the Mn^{2+} assay as described above, the surface area was calculated using the values of area per molecule shown in Table 1, and the lipid concentration was determined by ^{31}P NMR.

TABLE 1 Liposome-trapped water volumes, V_B, and areas per lipid molecule, A_L

Lipid	V_B* (μl/mg)	A_L# (Å^2)
18:0-18:1 PC	2.4 ± 0.3	66.6
18:0-18:1 PC, 1 M EtOH	2.6 ± 0.3	67.6
18:1-18:1 PC	2.7 ± 0.3	70.0
18:1-18:1 PC/18:1-18:1 PE	2.8 ± 0.3	67.6
18:0-18:3 PC	2.4 ± 0.2	66.6
18:0-22:6 PC	2.3 ± 0.2	71.6
18:0-22:6 PC, 1 M EtOH	2.1 ± 0.2	72.6
18:0-22:6 PC/18:1-18:1 PE	2.5 ± 0.3	70.8
22:6-22:6 PC	2.1 ± 0.2	76.6

*Lipid concentration was measured by ^{31}P NMR and trapped water volume by a Mn^{2+} assay.

#Data adapted from Rand and Parsegian (1989) and Separovic and Gawrisch (1996). In a recent study on 18:0-18:1 PC and 18:0-22:6 PC conducted at our laboratory, somewhat smaller areas per molecule have been determined (Koenig et al., manuscript submitted for publication).

The activation energy, E_A, for the permeation process was computed from the slope of a plot ln P_d versus $1/T$, according to

$$P_d(T) = P_0 e^{-(E_A/RT)} \quad (3)$$

RESULTS

Water permeability coefficients depend on accurate determination of trapped water volume (see Eq. 1). Liposomes are deformed by shear forces in the extrusion process (Clerc and Thompson, 1994). If extrusion is performed in an electrolyte solution, the liposomes remain nonspherical because water influx to convert liposomes into spheres would result in an osmotic stress gradient between inside and outside solutions, which is energetically unfavorable.

Liposome characterization

Liposome size

The size and shape characteristics of the extruded liposomes were measured by static and dynamic light scattering. All extruded liposome samples are found to have relatively narrow, unimodal, hydrodynamic diameter distributions. The mean liposome hydrodynamic diameter varied from 92 to 127 ± 36 nm. The diameter remained constant over a period of 72 h, which indicates that no vesicle aggregation or fusion occurred during preparation and measurement. Assuming an ellipsoidal shape for the liposomes as a model, the ratio of major to minor axes was calculated from the differences between static and dynamic light scattering. The resulting parameters yielded vesicle-entrapped volumes that agree with the trapped Mn^{2+} measurement reported below. The addition of 1 M ethanol does not influence the size and shape of extruded liposomes.

Trapped volume

The progress of liposome dialysis was monitored by determination of T_1 proton relaxation time for water in the dialysis solution. Dialysis was judged to be complete after ~18 h, indicated by no further increase in relaxation times. The ^{17}O NMR spin-spin relaxation time, T_{2A}, is very sensitive to traces of Mn^{2+} ions in the outer solution. The measured T_{2A} values indicate that the Mn^{2+} concentration in the outer solution was lowered by about three orders of magnitude during dialysis. Within experimental error, the T_{2A} values remained unchanged during the time course of the experiment, confirming that no leakage of Mn^{2+} ions had occurred. The amount of external Mn^{2+} that remained after dialysis was one to two orders of magnitude lower than the amount of trapped Mn^{2+} inside the liposomes and, therefore, did not perturb the measurement of liposome-trapped water volume. Values of trapped water volume (given in μl of trapped water per mg of lipid) are shown in Table 1. Typically, these values are ~20–40% smaller than volumes calculated assuming a spherical shape of the liposomes. There is a tendency for 18:1–18:1 PE-containing liposomes to have a larger trapped volume. Apparently these liposomes assume a shape that is less asymmetrical than those formed by pure PCs.

Unilamellarity of extruded liposomes

Liposomes extruded through 100-nm pores are reported to be unilamellar (Noy et al., 1995; Mui et al., 1993; Mayer et al., 1986). A control measurement was performed on 18:0–18:1 PC. The ^{31}P spectrum of extruded liposomes prepared in 72.9 mM NaCl solution was accumulated. Addition of 5 mM $MnCl_2$ broadened the phosphorus signal of the outer leaflet beyond detection. Integration of the remaining signal revealed that ~50% of the signal was eliminated, confirming that our liposomes are unilamellar.

Perturbation of lipid order due to the influence of Mn^{2+}

^{2}H NMR on sn-1 chain deuterated 16:0_{d31}-18:1 PC was employed to confirm that the addition of 50 mM $MnCl_2$ does not alter lipid packing. Fig. 2 shows the powder and de-Paked spectra of 16:0_{d31}-18:1 PC prepared in a) H_2O, b) 50 mM $MnCl_2$, and c) 50 mM $CaCl_2$. Within experimental error (±100 Hz), the ^{2}H NMR spectra in the presence of water and $MnCl_2$ are identical. However, the addition of 50 mM $CaCl_2$ resulted in a 5% order increase.

Membrane permeability

The ^{17}O NMR spin-spin relaxation times T_2, T_{2A}, and T_{2B} were measured as a function of temperature. Fig. 3 shows the temperature dependence of all three relaxation times for a 1 wt% 18:0–22:6 PC preparation. The values for T_{2A} are slightly shorter than values for pure 72.9 mM NaCl solution because of traces of Mn^{2+} that have not been removed during dialysis. T_{2B} of the water signal in the internal pool (Fig. 3 *B*) is also reduced by binding of water molecules to the lipid surface. Bound water molecules have longer mo-

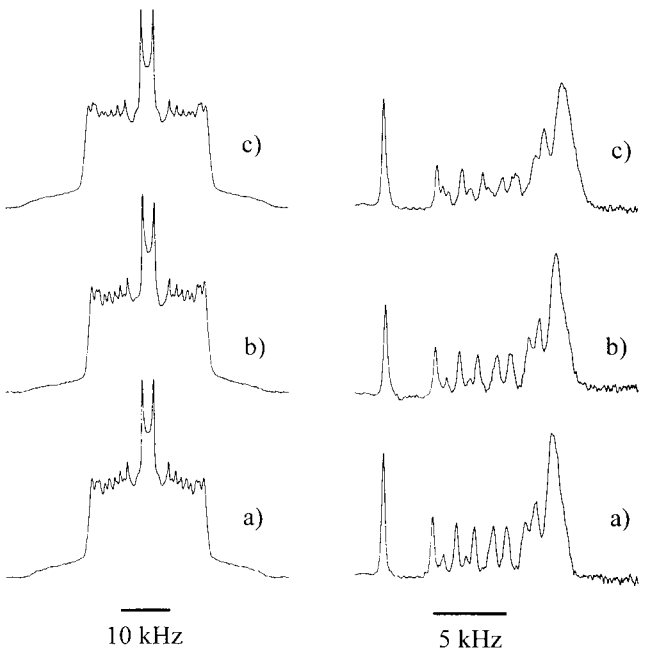

FIGURE 2 ^{2}H NMR powder spectra (*left*) and de-Paked spectra (*right*) of 16:0_{d31}-18:1 PC at 25°C. Lipids were prepared in water (*a*), 50 mM $MnCl_2$ (*b*), and 50 mM $CaCl_2$ (*c*). The addition of 50 mM Mn^{2+} did not change quadrupolar splitting; however, 50 mM Ca^{2+} increased the hydrocarbon chain order by 5%.

tional correlation times, which translates into shorter relaxation times. Therefore, for the measurement of the internal relaxation time, T_{2B}, the lipid/water ratio had to be adjusted, reproducing exactly the environment inside of a liposome (210 water molecules per lipid of the inner leaflet for 18:0–18:1 PC). T_{2A} becomes longer with increasing temperature because of shorter water correlation times at higher temperatures. T_2, however, decreases with increasing temperature, indicating the fast exchange of water across the membrane and the related loss of magnetization due to much faster relaxation inside the liposomes (Eq. 1).

Lipid bilayers are generally characterized by very low permeability to mono- and divalent ions. However, a dramatic increase in the permeability of ions occurs at the phase transition from gel to liquid-crystalline (Mouritsen et al., 1995; Papahadjopoulos et al., 1973). Our permeability measurements were conducted well above the phase transition temperature of the lipids to avoid leakage of Mn^{2+}.

Acyl chain unsaturation

Fig. 4 shows the influence of chain unsaturation and temperature on water permeability. Permeability coefficients increase drastically with the introduction of more double bonds from 155 ± 24 μm/s for 18:0–18:1 PC to 662 ± 189 μm/s for 22:6–22:6 PC at 25°C. The permeability coefficients of 18:0–18:3 PC and 18:0–22:6 PC are about a factor of 3 higher then those of 18:0–18:1 PC, but no significant differences between the two polyunsaturated lipids were found. Activation energies of water permeability, E_A, increase slightly with increasing unsaturation.

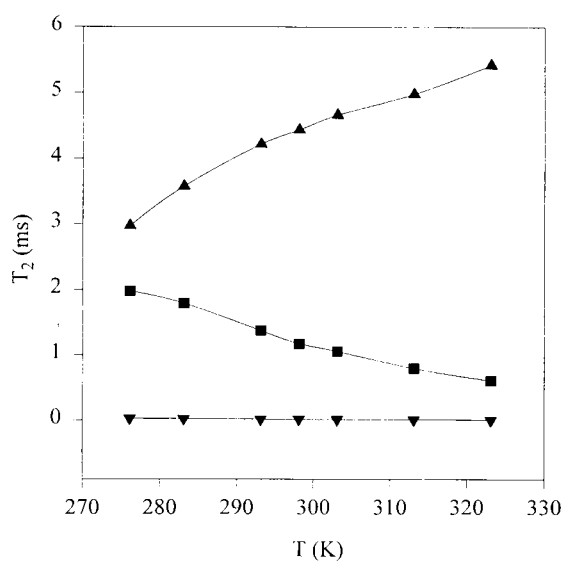

FIGURE 3 Spin-spin relaxation times (T_2, ■; T_{2A}, ▲; T_{2B}, ▼) used for the calculation of water lifetime inside liposomes according to Eq. 1 (sample: 18:0–22:6 PC). The precision of calculated permeation rates increases with increasing difference between T_2 (■) and T_{2A} (▲). However, when T_2 (■) approaches T_{2B} (▼), the error in the value of T_{2B} becomes more significant for the determination of the average lifetime of water inside the liposomes, τ_B.

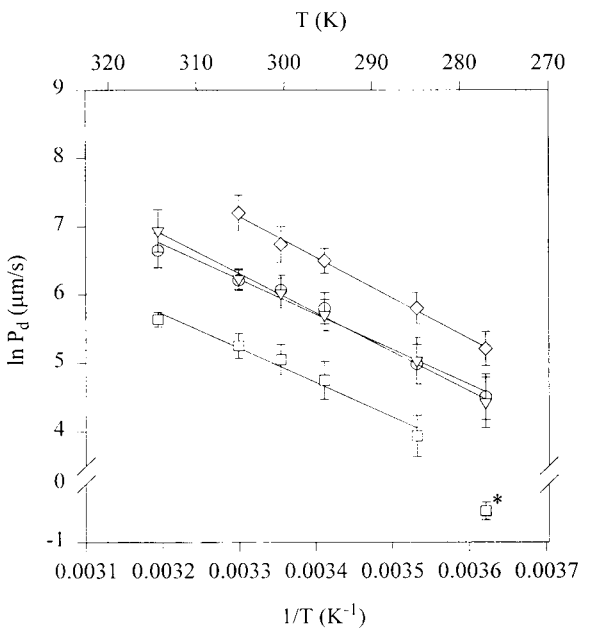

FIGURE 4 Permeation coefficients versus temperature for lipids with varying degrees of unsaturation. According to this plot, 18:0–18:1 PC (□) membranes are least permeable to water, followed by 18:0–18:3 PC (○), 18:0–22:6 PC (▽), and 22:6–22:6 PC (◇) bilayers. According to Eq. 3, the slopes of the fitted lines give the respective activation energies. The data point marked with the star represents the permeability of 18:0–18:1 PC in the L_β phase measured by using the spin-lattice relaxation times of the ^{1}H signal of water.

The data point highlighted with a star in Fig. 4 represents a T_1 measurement of the ^{1}H NMR signal of water of a 18:0–18:1 PC preparation at 276.1 K according to the method of Andrasko and Forsen (1974). At this temperature 18:0–18:1 PC is in the gel phase (Niebylski and Salem, 1994), where water permeability is much lower (Jansen and Blume, 1995; Fettiplace and Haydon, 1980). We calculated a lifetime of water inside the vesicles of $\tau_B = 18 \pm 3$ ms and a permeability coefficient of $P_d = 0.62 \pm 0.15$ μm/s. Permeability coefficients of this magnitude cannot be measured with the ^{17}O NMR method, because the difference in the linewidth is too small to be resolved.

Water permeability of PC/ethanol mixtures

The influence of ethanol on water permeability is shown in Fig. 5. The addition of 1 M ethanol decreases permeability coefficients of 18:0–18:1 PC to almost half of the value measured in the absence of ethanol. The same effect is observed for the highly unsaturated 18:0–22:6 PC. Measurement of the permeability coefficient began at 15°C to prevent vesicle fusion, which may occur in the presence of ethanol at lower temperatures (Komatsu and Okada, 1995). Ethanol slightly reduces the thermal activation energy of water permeation. The reduction is larger for 18:0–22:6 PC than for 18:0–18:1 PC.

Water permeability of PC/PE mixtures

Water permeability of 18:1–18:1 PC/18:1–18:1 PE mixtures (1/1, mol/mol) is significantly reduced in comparison to pure 18:1–18:1 PC bilayers, as shown in the two lower curves in Fig. 6. Activation energy of water permeation increases from 9.9 kcal/mol for pure 18:1–18:1 PC to 12.9 kcal/mol for the mixture. In contrast, water permeation of 18:1–22:6 PC remains almost unperturbed by the presence of equimolar 18:1–18:1 PE.

Finally, the lifetime of water inside the vesicles and the permeability coefficients at temperatures from 5°C to 40°C were calculated for all nine lipid preparations; these are shown in Table 2.

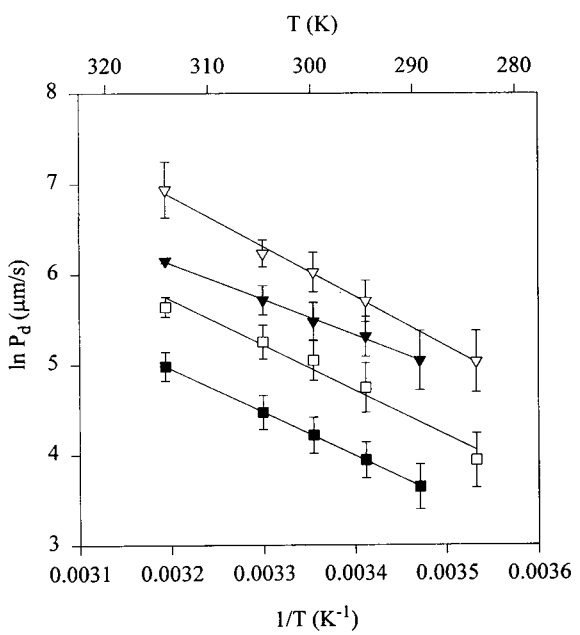

FIGURE 5 Permeability coefficients of 18:0–18:1 PC (□, ■) and 18:0–22:6 PC (▽, ▼) with (■, ▼) and without (□, ▽) 1 M ethanol versus temperature. The addition of 1 M ethanol decreases water permeation through bilayers of monounsaturated and polyunsaturated lipids.

DISCUSSION

The permeation results support the hypothesis that water permeability across polyunsaturated bilayers is significantly higher than across saturated and monounsaturated bilayers. Measurements on polyunsaturated membranes are challenging because of lipid sensitivity to oxidation and special requirements of the experimental method for measuring short lifetimes of water inside liposomes. The ^{17}O NMR method with Mn^{2+} ions trapped inside liposomes, initially used by Lipschitz-Farber and Degani (1980) on sonicated small unilamellar liposomes, is very well suited for measurement of fast water permeation through highly unsaturated phospholipid bilayers. Permeation measurements on liposomes "loaded" with Mn^{2+} ions have the highest sen-

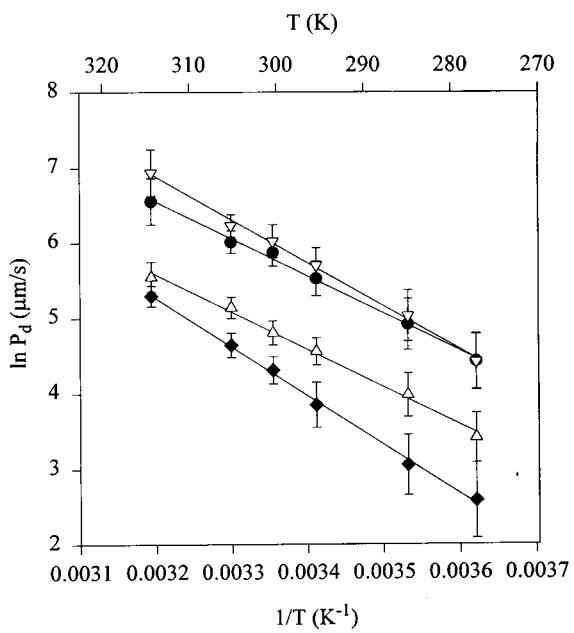

FIGURE 6 Influence of 18:1–18:1 PE on water permeability. The lower two curves represent the permeability coefficients of 18:1–18:1 PC (△) and 18:1–18:1 PC/18:1–18:1 PE (1/1 mol/mol) (◆). Permeability coefficients of the mixture are 20–70% smaller than those of pure PC. The activation energy of water permeation for the 18:1–18:1 PC/18:1–18:1 PE mixture is somewhat higher than for pure 18:1–18:1 PC. No significant difference in permeability coefficients was detected between 18:0–22:6 PC (▽) and a 18:0–22:6 PC/18:1–18:1 PE (1/1 mol/mol) mixture (●), as shown in the upper two curves. The thermal activation energy for the 18:0–22:6 PC/18:1–18:1 PE mixture is slightly smaller than that for pure 18:0–22:6 PC.

TABLE 2 Lifetimes of water inside the vesicles, τ_B, permeability coefficients, P_d, and the thermal activation energies, E_A

Lipid	Temperature (°C)	τ_B* (μs)	P_d* (μm/s)	E_A# (kcal/mol)
18:0-18:1 PC	10	193 ± 38	51 ± 18	
	25	63 ± 9	155 ± 24	9.9 ± 0.8
	40	35 ± 3	279 ± 31	
18:0-18:1 PC, 1 M EtOH	15	275 ± 46	38 ± 11	
	25	152 ± 23	66 ± 15	9.5 ± 0.7
	40	74 ± 9	143 ± 25	
18:0-18:3 PC	10	67 ± 9	145 ± 47	
	25	23 ± 3	330 ± 88	10.2 ± 0.7
	40	13 ± 4	771 ± 199	
18:0-22:6 PC	10	61 ± 8	153 ± 58	
	25	23 ± 3	412 ± 91	10.9 ± 0.5
	40	9 ± 3	1030 ± 305	
18:0-22:6 PC, 1 M EtOH	15	54 ± 5	155 ± 49	
	25	35 ± 3	239 ± 67	7.8 ± 0.8
	40	18 ± 3	469 ± 99	
22:6-22:6 PC	10	25 ± 4	331 ± 69	
	25	10 ± 2	662 ± 189	11.8 ± 1.0
	40	6 ± 2	1334 ± 756	
18:1-18:1 PC	10	197 ± 33	53 ± 18	
	25	86 ± 8	122 ± 21	9.9 ± 0.7
	40	41 ± 4	257 ± 29	
18:1-18:1 PC/18:1-18:1 PE	10	518 ± 255	21 ± 12	
	25	152 ± 17	74 ± 15	12.8 ± 0.3
	40	55 ± 7	199 ± 30	
18:0-22:6 PC/18:1-18:1 PE	10	73 ± 8	136 ± 57	
	25	30 ± 3	335 ± 91	9.8 ± 0.2
	40	14 ± 2	701 ± 277	

*The errors were calculated considering errors in T_2 determination, lipid concentration, and internal volume. Permeability measurements have the highest precision for water lifetimes inside liposomes from 15 to 150 μs, translating into permeability coefficients of 70–700 μm/s.
#The activation energy error was calculated from the standard deviation of experimental data points to the linear fit of ln P_d versus $1/T$.

sitivity, at lipid concentrations near 1–2 wt%. Extrusion at such low lipid concentration results in more uniform unilamellar liposomes with less tendency for aggregation, fusion, or leakage of internal electrolyte.

Measurement of fast water exchange, as in the case of polyunsaturated membranes, requires short relaxation times, T_{2B}. This can be achieved with a high concentration of relaxation agent (Koenig et al., 1992) or, as in our experiments, by observing the resonance signal of natural-abundance ^{17}O in water, which is more sensitive to the presence of paramagnetic ions. T_2 relaxation times have been determined by fitting the ^{17}O resonance lineshape with a Lorentzian function. Resonance lines appear to be homogeneously broadened, and a linewidth analysis results in smaller experimental errors than a measurement of T_2 relaxation times by a Carr-Purcell-Meiboom-Gill pulse sequence. ^{17}O NMR experiments must be conducted with proton decoupling to remove unresolved scalar coupling between water protons and oxygen ($^1J_{OH} \approx 90$ Hz), which broadens the ^{17}O resonance line (Earl and Niederberger, 1977; Burnett and Zeltmann, 1974).

Because divalent ions bind to neutral lipid surfaces (Lis et al., 1981a,b), the influence of the paramagnetic Mn^{2+} ions on the lipid chain order was measured. Although it was reported that Ca^{2+} and Mn^{2+} bind to about the same extent to 16:0–16:0 PC (Lis et al., 1981a), lipid chain order is not influenced by Mn^{2+}, but is increased because of Ca^{2+}. We conclude from this measurement that the 50 mM $MnCl_2$ solution is unlikely to influence the permeability measurement.

The value of water permeability coefficients depends critically on accurate determination of trapped water volume. In previous investigations, trapped water volume has been determined from average liposome size, assuming that the liposomes are spheres (Jansen and Blume, 1995; Koenig et al., 1992; Spineni et al., 1983; Haran and Shporer, 1976). However, it has been shown by others (White et al., 1996; Mui et al., 1993; Clerc and Thompson, 1994; Lichtenberg et al., 1981), and was confirmed in this study, that extruded liposomes are nonspherical, resulting in an internal water volume that is 20–40% lower than that of a spherical particle with identical hydrodynamic radius. This may explain why our calculated water permeation coefficients for monounsaturated lipids are slightly higher than values published previously (Koenig et al., 1992; Haran and Shporer, 1976; Reeves and Dowben, 1970). Our values for 18:1–18:1 PC and 18:0–18:1 PC are in excellent agreement with recently published data by Paula et al. (1996).

Water permeability and unsaturation

Increasing lipid hydrocarbon chain unsaturation enhances diffusion-controlled water permeability of phospholipid bi-

layers. Increased rates of water permeation are related to differences in lipid packing. This general rule does not apply to the transition from 18:0–18:3 PC to the more unsaturated 18:0–22:6 PC, where more unsaturation results in a marginal increase of permeability coefficients only. The sixfold unsaturated docosahexaenoic acid chain (22:6) has four more carbon atoms than the three-fold unsaturated α-linolenic acid. Most likely the degree of unsaturation and the chain length of the unsaturated chain determine water permeation rates.

As revealed by ^{2}H NMR order parameter profiles, the sn-1 chain exhibits a selective increase in motional freedom in a region located toward the bottom half of the chain as sn-2 unsaturation increases (Holte et al., 1995). This corresponds to an area increase around carbon atom 14 that is three to four times greater than the increase for the top part of the chain, and may result in an interface regime that is less tightly packed. Thus the capability of water to penetrate the lipid-water interface may be enhanced for polyunsaturated lipids, resulting in increased water permeability. This model is supported by molecular dynamics studies on lipid bilayers. In these simulations the area occupied by glycerol and the upper part of lipid hydrocarbon chains exerts the main resistance to water permeation, because of higher free energy and lower diffusion rates of water (Marrink and Berendsen, 1994, 1996; Marrink and Berkowitz, 1995). We suggest that polyunsaturation lowers resistance to water permeation in the critical upper third of lipid hydrocarbon chains.

Influence of the ethanolamine headgroup

PEs have higher chain order than PCs (Lafleur et al., 1990; Sternin et al., 1988). The chain order of PCs increases when PEs are added to the mixture (Barry and Gawrisch, manuscript submitted for publication; Separovic and Gawrisch, 1996; Fenske et al., 1990; Lafleur et al., 1989, 1990). Order increase with addition of PE to PC is biggest in mixtures of saturated and monounsaturated lipids and much smaller for polyunsaturated lipids (Barry and Gawrisch, manuscript submitted for publication; Separovic and Gawrisch, 1996). Increased order is equivalent to higher lipid packing density and smaller area per molecule (Separovic and Gawrisch, 1996), which reduces interchain water concentration, as observed in fluorescence measurements (Stubbs et al., 1995). In good agreement with these observations, water permeation is significantly lower in equimolar mixtures of 18:1–18:1 PC/18:1–18:1 PE, and somewhat lower in 18:0–22:6 PC/18:1–18:1 PE.

Water permeability and ethanol

Whereas polyunsaturation reduces hydrocarbon chain order and increases water permeation, the addition of 1 M ethanol also reduces hydrocarbon chain order but reduces water permeation rates. Fluorescence measurements performed by Stubbs and colleagues (Boni et al., 1993) suggest that water concentration increases in membranes containing ethanol, therefore eliminating the possibility that lower water concentration inside the membrane hydrophobic core limits water permeation. However, ethanol may also reduce water permeation by restricting entry of water molecules into the bilayer. Because of its amphipathic nature, an ethanol molecule has the lowest free energy when located at the lipid water interface. In recent NMR investigations we measured ethanol location in bilayers by two-dimensional NOESY spectroscopy and summarized results as an ethanol distribution function (Holte and Gawrisch, 1997). Ethanol concentration is highest at the lipid-water interface near the glycerol and decreases toward the center of the bilayer and the upper end of headgroups. We hypothesize that ethanol limits the dynamic access of water molecules to the bilayer by blocking diffusion pathways of water into the membrane core.

CONCLUSIONS

We observed that perturbation of lipid packing by chain polyunsaturation and headgroup composition, as well as modifications of the lipid-water interface region by ethanol, influence diffusion-controlled water permeability. The activation energy of water permeation in the range of 8–12 kcal/mol, measured in this study, is much higher than the 4.6 kcal/mol characterizing the self-diffusion of water (Wang et al., 1953) and higher than the 4–6 kcal of activation energy for water permeation through the CHIP 28 pores in erythrocyte membranes (Benga, 1994). The higher values suggest that water molecules interact with the lipid matrix during the course of water transit, which is in better agreement with the solubility diffusion model of water permeation (Finkelstein and Cass, 1968; Hanai and Haydon, 1966) than with the hypothesis of water diffusion through pores.

In its recent modification, called the *inhomogeneous solubility-diffusion model*, the complexity of a phospholipid membrane is reproduced by dividing the membrane into four regions with different properties of membrane-solubilized water (Marrink and Berendsen, 1994, 1996; Marrink and Berkowitz, 1995). Resistance to water permeation is highest in the area containing the upper hydrocarbon chains. Lower chain order as a result of chain unsaturation (Holte et al., 1995) correlates with increased water permeation, whereas higher order, as in PE-containing membranes (Separovic and Gawrisch, 1996), decreases permeation rates. The lower water permeation rates in the presence of ethanol can be explained with a model whereby ethanol and water compete for identical polar binding sites in the lipid-water interface region.

The authors thank Judith A. Barry, Lev D. Bergelson, Laura L. Holte, Ralph Nossal, and Nils Olsson for helpful discussions. Preliminary proton experiments for this study were conducted by Aaron Snyder. The light

scattering measurements were carried out in the Laboratory of Molecular Biology, NIDDK, National Institutes of Health.

DH is grateful for a grant by the Studienstiftung des deutschen Volkes and support by the Deutsche Forschungsgemeinschaft (SFB 197).

REFERENCES

Andrasko, J., and S. Forsen. 1974. NMR study of rapid water diffusion across lipid bilayers in dipalmitoyl lecithin vesicles. *Biochem. Biophys. Res. Commun.* 60:813–819.

Barry, J. A., and K. Gawrisch. 1994. Direct NMR evidence for ethanol binding to the lipid-water interface of phospholipid bilayers. *Biochemistry.* 33:8082–8088.

Barry, J. A., and K. Gawrisch. 1995. Effects of ethanol on lipid bilayers containing cholesterol, gangliosides, and sphingomyelin. *Biochemistry.* 34:8852–8860.

Benga, G. 1994. Water channels in membranes. *Cell Biol. Int.* 18: 829–833.

Boni, L. T., S. R. Minchey, W. R. Perkins, P. L. Ahl, J. L. Slater, M. W. Tate, S. M. Gruner, and A. S. Janoff. 1993. Curvature dependent induction of the interdigitated gel phase in DPPC vesicles. *Biochim. Biophys. Acta.* 1146:247–257.

Burnett, L. J., and A. H. Zeltmann. 1974. ^{1}H-^{17}O spin-spin coupling constant in liquid water. *J. Chem. Phys.* 60:4636–4637.

Clerc, S. G., and T. E. Thompson. 1994. A possible mechanism for vesicle formation by extrusion [letter; comment]. *Biophys. J.* 67:475–476.

Colman, A., and D. G. Gadian. 1976. ^{31}P nuclear-magnetic-resonance studies on the developing embryos of *Xenopus laevis*. *Eur. J. Biochem.* 61:387–396.

Conlon, T., and R. Outhred. 1972. Water diffusion permeability of erythrocytes using an NMR technique. *Biochim. Biophys. Acta.* 288:354–361.

Davis, J. H., K. R. Jeffrey, M. Bloom, M. I. Valic, and T. P. Higgs. 1976. Quadrupolar echo deuteron magnetic resonance spectroscopy in ordered hydrocarbon chains. *Chem. Phys. Lett.* 42:390–394.

Deamer, D. W., and J. Bramhall. 1986. Permeability of lipid bilayers to water and ionic solutes. *Chem. Phys. Lipids.* 40:167–188.

Disalvo, E. A., F. A. Siddiqi, and H. T. Tien. 1989. Membrane transport with emphasis on water and non-electrolytes in experimental lipid bilayers and biomembranes. *In* Water Transport in Biological Membranes. G. Benga, editor. CRC Press, Boca Raton, FL.

Earl, W. L., and W. Niederberger. 1977. Proton decoupling in ^{17}O nuclear magnetic resonance. *J. Magn. Reson.* 27:351–353.

Fenske, D. B., and P. R. Cullis. 1993. Acyl chain orientational order in large unilamellar vesicles: comparison with multilamellar liposomes: a ^{2}H and ^{31}P nuclear magnetic resonance study. *Biophys. J.* 64: 1482–1491.

Fenske, D. B., H. C. Jarell, Y. Guo, and S. W. Hui. 1990. Effect on unsaturated phosphatidylethanolamine on the chain order profile of bilayers at the onset of the hexagonal phase transition. A ^{2}H NMR study. *Biochemistry.* 29:11222–11229.

Fettiplace, R., and D. A. Haydon. 1980. Water permeability of lipid membranes. *Physiol. Rev.* 60:510–550.

Finkelstein, A. 1987. Water Movement Through Lipid Bilayers, Pores, and Plasma Membranes. John Wiley and Sons, New York.

Finkelstein, A., and P. Cass. 1968. Permeability and electrical properties of thin lipid membranes. *J. Gen. Physiol.* 52:145s–172s.

Haines, T. H., and L. S. Liebovitch. 1995. A molecular mechanism for the transport of water across phospholipid bilayers. *In* Permeability and Stability of Lipid Bilayers. E. A. Disalvo and S. A. Simon, editors. CRC Press, Boca Raton, FL. 123–136.

Hanai, T., and D. A. Haydon. 1966. The permeability to water of biomolecular lipid membranes. *J. Theor. Biol.* 11:370–382.

Haran, N., and M. Shporer. 1976. Study of water permeability through phospholipid vesicle membranes by ^{17}O NMR. *Biochim. Biophys. Acta.* 426:638–646.

Ho, C., S. J. Slater, and C. D. Stubbs. 1995. Hydration and order in lipid bilayers. *Biochemistry.* 34:6188–6195.

Holte, L. L., and K. Gawrisch. 1997. Determining ethanol distribution in phospholipid multilayers with MAS-NOESY spectra. *Biochemistry.* 36: 4669–4674.

Holte, L. L., S. A. Peter, T. M. Sinnwell, and K. Gawrisch. 1995. ^{2}H nuclear magnetic resonance order parameter profiles suggest a change of molecular shape for phosphatidylcholines containing a polyunsaturated acyl chain. *Biophys. J.* 68:2396–2403.

Hope, M. J., M. B. Bally, G. Webb, and P. R. Cullis. 1985. Production of large unilamellar vesicles by a rapid extrusion procedure. Characterization of size distribution, trapped volume and ability to maintain a membrane potential. *Biochim. Biophys. Acta.* 812:55–65.

Inoue, T., H. Kamaya, and I. Ueda. 1985. Alcohol effects on rapid kinetics of water transport through lipid membranes and location of the main barrier. *Biochim. Biophys. Acta.* 815:68–74.

Jansen, M., and A. Blume. 1995. A comparative study of diffusive and osmotic water permeation across bilayers composed of phospholipids with different head groups and fatty acyl chains. *Biophys. J.* 68: 997–1008.

Koenig, S. H., F. A. Quet, R. D. Brown, M. Lafleur, M. Spiller, E. Unger, and C. Tilcock. 1992. Permeability of liposomal membranes to water: result from the magnetic field dependence of T_1 of solvent protons in suspension of vesicles with entrapped paramagnetic ions. *Magn. Reson. Med.* 23:275–286.

Komatsu, H., and S. Okada. 1995. Ethanol-induced aggregation and fusion of small phosphatidylcholine liposomes: participation of interdigitated membrane formation in their processes. *Biochim. Biophys. Acta.* 1235: 270–280.

Lafleur, M., P. R. Cullis, B. Fine, and M. Bloom. 1990. Comparison of the orientational order of lipid chains in the L_α and H_{II} phases. *Biochemistry.* 29:8325–8333.

Lafleur, M., B. Fine, E. Sternin, P. R. Cullis, and M. Bloom. 1989. Smoothed orientational order profile of lipid bilayers by ^{2}H-nuclear magnetic resonance. *Biophys. J.* 56:1037–1041.

Lahajnar, G., P. Macek, P. Smid, and I. Zupancic. 1995. Ethanol- and acetonitrile-induced inhibition of water diffusional permeability across bovine red blood cell membrane. *Biochim. Biophys. Acta.* 1235: 437–442.

Lichtenberg, D., E. Freire, C. F. Schmidt, Y. Barenholz, P. L. Felgner, and T. E. Thompson. 1981. Effect of surface curvature on stability, thermodynamic behavior, and osmotic activity of dipalmitoylphosphatidylcholine single lamellar vesicles. *Biochemistry.* 20:3462–3467.

Lipschitz-Farber, D., and H. Degani. 1980. Kinetics of water diffusion across phospholipid membranes. ^{1}H- and ^{17}O-NMR relaxation studies. *Biochim. Biophys. Acta.* 600:291–300.

Lis, L. J., W. T. Lis, V. A. Parsegian, and R. P. Rand. 1981a. Adsorption of divalent cations to a variety of phosphatidylcholine bilayers. *Biochemistry.* 20:1771–1777.

Lis, L. J., V. A. Parsegian, and R. P. Rand. 1981b. Binding of divalent cations of dipalmitoylphosphatidylcholine bilayers and its effect on bilayer interaction. *Biochemistry.* 20:1761–1770.

Marrink, S.-J., and H. J. C. Berendsen. 1994. Simulation of water transport through a lipid membrane. *J. Phys. Chem.* 98:4155–4168.

Marrink, S.-J., and H. J. C. Berendsen. 1996. Permeation process of small molecules across lipid membranes studies by molecular dynamics simulation. *J. Phys. Chem.* 100:16729–16738.

Marrink, S.-J., and M. Berkowitz. 1995. Water and membranes. *In* Permeability and Stability of Lipid Bilayers. E. A. Disalvo and S. A. Simon, editors. CRC Press, Boca Raton, FL. 21–48.

Mayer, L. D., M. J. Hope, and P. R. Cullis. 1986. Vesicles of variable sizes produced by a rapid extrusion procedure. *Biochim. Biophys. Acta.* 858: 161–168.

Mouritsen, O. G., K. Jørgensen, and T. Hønger. 1995. Permeability of lipid bilayers near the phase transition. *In* Permeability and Stability of Lipid Bilayers. E. A. Disalvo and S. A. Simon, editors. CRC Press, Boca Raton, FL. 137–160.

Mui, B. L.-S., P. R. Cullis, E. A. Evans, and T. D. Madden. 1993. Osmotic properties of large unilamellar vesicles prepared by extrusion. *Biophys. J.* 64:443–453.

Niebylski, C., and N. J. Salem. 1994. A calorimetric investigation of a series of mixed-chain polyunsaturated phosphatidylcholines: effect of sn-2 chain length and degree of unsaturation. *Biophys. J.* 67:2387–2393.

Noy, N., D. J. Kelleher, and A. W. Scotto. 1995. Interactions of retinol with lipid bilayers: studies with vesicles of different radii. *J. Lipid Res.* 36:375–382.

Papahadjopoulos, D., K. Jacobson, S. Nir, and T. Isac. 1973. Phase transition in phospholipid vesicles. Fluorescence polarization and permeability measurements concerning the effect of temperature and cholesterol. *Biochim. Biophys. Acta.* 311:330–348.

Paula, S., A. G. Volkov, A. N. Van Hoek, T. H. Haines, and D. W. Deamer. 1996. Permeation of protons, potassium ions, and small polar molecules through phospholipid bilayers as a function of membrane thickness. *Biophys. J.* 70:339–348.

Rand, R. P., and V. A. Parsegian. 1989. Hydration forces between phospholipid bilayers. *Biochim. Biophys. Acta.* 988:351–376.

Reeves, J. P., and R. M. Dowben. 1970. Water permeability of phospholipid vesicles. *J. Membr. Biol.* 3:123–141.

Seeman, P., R. I. Sha'afi, W. R. Galey, and A. K. Solomon. 1970. The effect of anesthetics (chlorpromazine, ethanol) on erythrocyte permeability to water. *Biochim. Biophys. Acta.* 211:365–368.

Separovic, F., and K. Gawrisch. 1996. The effect of unsaturation on chain order of phosphatidylcholines in a DOPE matrix. *Biophys. J.* 71: 274–282.

Simon, S. A., and T. J. McIntosh. 1986. Depth of water penetration into lipid bilayers. *Methods Enzymol.* 127:511–521.

Slater, S. J., C. Ho, F. J. Taddeo, M. B. Kelly, and C. D. Stubbs. 1993. Contribution of hydrogen bonding to lipid-lipid interactions in membranes and the role of lipid order: effects of cholesterol, increased phospholipid unsaturation, and ethanol. *Biochemistry.* 32:3714–3721.

Spineni, J. P., R. Grosescu, M. Lupu, and V. Dobre. 1983. ^{1}H-NMR relaxation study of cholesterol effect on water diffusion across phospholipid vesicle membranes. *Rev. Roum. Biochim.* 20:271–277.

Sternin, E., M. Bloom, and A. L. MacKay. 1983. De-pake-ing of NMR spectra. *J. Magn. Reson.* 55:274–282.

Sternin, E., B. Fine, M. Bloom, C. P. Tilcock, K. F. Wong, and P. R. Cullis. 1988. Acyl chain orientational order in the hexagonal H_{II} phase of phospholipid-water dispersions. *Biophys. J.* 54:689–694.

Straume, M., and B. J. Litman. 1987. Equilibrium and dynamic structure of large, unilamellar, unsaturated acyl chain phosphatidylcholine vesicles. Higher order analysis of 1,6-diphenyl-1,3,5-hexatriene and 1-[4-(trimethylamonio)phenyl]-6-phenyl-1,3,5-hexatriene anisotropy decay. *Biochemistry.* 26:5113–5120.

Stubbs, C. D., C. Ho, and S. J. Slater. 1995. Fluorescence techniques for probing water penetration into lipid bilayers. *J. Fluoresc.* 5:19–28.

Swift, T. J., and R. E. Connick. 1962. NMR-relaxation mechanism of ^{17}O in aqueous solution of paramagnetic cations and the lifetime of water molecules in the first coordination sphere. *J. Chem. Phys.* 37:307–320.

Taraschi, T. F., A. Wu, and E. Rubin. 1985. Phospholipid spin probes measure the effect of ethanol on the molecular order of liver microsomes. *Biochemistry.* 24:7096–7101.

Thurmond, R. L., S. W. Dodd, and M. F. Brown. 1991. Molecular areas of phospholipids as determined by ^{2}H NMR spectroscopy. Comparison of phosphatidylethanolamines and phosphatidylcholines. *Biophys. J.* 59: 108–113.

Wang, J. H., C. V. Robinson, and I. S. Edelman. 1953. Self diffusion and structure of liquid water. III. Measurement of the self-diffusion of liquid water with ^{2}H, ^{3}H, and ^{18}O as tracers. *J. Am. Chem. Soc.* 75:466–470.

White, G., J. Pencer, B. G. Nickel, J. M. Wood, and F. R. Hallett. 1996. Optical changes in unilamellar vesicles experiencing osmotic stress. *Biophys. J.* 71:2701–2715.

Wiener, M. C., and S. H. White. 1992. Structure of a fluid dioleoylphosphatidylcholine bilayer determined by joint refinement of x-ray and neutron diffraction data. III. Complete structure. *Biophys. J.* 61: 434–447.

Ye, R., and A. S. Verkman. 1989. Simultaneous optical measurement of osmotic and diffusional water permeability in cells and liposomes. *Biochemistry.* 28:824–829.